Sound & Vibration 2026, 60(4), 4028.
doi: https://doi.org/10.59400/sv4028

Article

A framework of structural health monitoring integrated with deep learning schemes to estimate the displacement of 3D LiDAR scanning on bridges

Wael A. Altabey

Department of Mechanical Engineering, Faculty of Engineering, Alexandria University, Alexandria 21544, Egypt; wael.altabey@gmail.com

CITATION

Altabey WA. A framework of structural health monitoring integrated with deep learning schemes to estimate the displacement of 3D LiDAR scanning on bridges. Sound & Vibration. 2026; 60(4): 4028. https://doi.org/10.59400/sv4028

ARTICLE INFO

Received: 10 February 2026
Revised: 10 April 2026
Accepted: 14 April 2026
Available online: 30 June 2026

Abstract: In recent decades, the rapid development of transportation infrastructure safety, such as highways, bridges, and tunnels has greatly promoted the development of the regional economy. The structures with safety hazards and emergencies need continuous monitoring over time. The integrated artificial intelligence algorithms with sensor responses can provide real-time information for further analysis and decision-making for the transportation system, improving the circulation efficiency of the transportation network, ensuring the stability of road structures, and avoiding irreparable damage. This paper aims to develop an efficient and low-cost method to help detect early-stage transportation infrastructure damage through permanent or periodic monitoring. In this research, we used LiDAR scanning units (terrestrial LiDAR fixed on holders and movable units fixed on UAVs) integrated with a novel deep neural network (DNN) for structural monitoring of bridges based on the 3D mapping of bridge displacement compiled from LiDAR scanning over time. The monitoring model is based on a recurrent neural network with long short-term memory blocks (RNN-LSTM) since the LiDAR scanning datasets have a time-dependent and memory-dependent behavior. The response of the proposed DNN achieved a high accuracy rate, regression rate, and F-score equal to 96.43%, 93.77%, and 91.65%, respectively. A deep analysis of the confusion matrix and a side-by-side look at predicted and actual conditions highlight how well the model can tell apart different traditional methods to estimate the bridge displacement in literature. So, the data from LiDAR and DNN models can be combined to analyze the monitoring of transportation infrastructure.

Keywords: structural health monitoring; LiDAR scanning; bridge displacement; deep learning; recurrent neural network; long short-term memory blocks

1. Introduction

People generally expect a safe and convenient travel experience in the transportation industry. For safety in transportation systems, there's a need to focus on preventive maintenance and safety checks of infrastructure. It should be keeping a monitoring on how things are performing over time, improving how we gather data, and upgrading our testing and maintenance technology. Furthermore, adopting new materials and tech can help us make better infrastructure that lasts longer [1].

With more mountain highways being built, there are lots of bridges popping up along the routes, making bridge safety inspections super important for keeping the highways in good shape. Right now, these inspections mostly depend on manual checks, and there are quite a few challenges to deal with, especially since it can be slow and inefficient [2], due to the subjective nature of visual assessments, which isn't

always reliable, especially when it comes to special structures that need regular checks, Human eyes can only do so much, especially when inspections require climbing to tough spots [3]. Managers face a big task here: they need to find a way to manage these bridges better, create solid plans, and keep track of their health in real-time. Ensuring safety is crucial for people's lives and property [4].

Measuring a structural displacement is really important for construction because it's one of the main points to check the structural safety. Understanding the displacement of structures can estimate the load-carrying capacity of bridges, figure out the dynamic characteristics of structures, and improve the structure's finite element model. There are various methods to measure this displacement, which can be divided into two main types: contact and non-contact techniques [5]. Common contact sensors include accelerometers [6], strain gauges [7], inclinometers [8], and global navigation satellite systems (GNSS) [9, 10]. But there are some drawbacks with accelerometers—they often deal with significant low-frequency drift or miss out on crucial low-frequency data. Furthermore, using strain gauges and inclinometers usually requires installing a lot of sensors, even if trying to get a reading from one point.

LiDAR, which stands for light detection and ranging, is a useful tool for measuring displacement without any contact. It figures out how far away something is by using either the time of flight (ToF) method or a phase-based approach [11, 12]. After that, it calculates the displacement based on the change in distance. One of the things about LiDAR, compared to other methods of noncontact instruments, is that it can capture 3D displacement and is less affected by lighting conditions. Furthermore, unlike vision-based methods that need a scale factor to change capture area movement in pixels to actual physical displacement, LiDAR can measure displacement directly in physical length units. This makes calculations a lot easier.

Terrestrial LiDAR has proven that it is effective for checking structures and measuring deformation. He et al. [13] along with Tan et al. [14] confirmed that terrestrial LiDAR is accurate enough for monitoring bridge deformations in real-time. Artese et al. [15] established a comprehensive method that combined a terrestrial LiDAR, and finite element analysis, which they then used to evaluate medieval masonry bridges. Sedek and Serwa [16] showcased the strong potential of terrestrial LiDAR for identifying building defects, ensuring quality control, and tracking spatial deformations. Park et al. [17] used terrestrial LiDAR to monitor the steel beams' deformation, and managed to provide deformation data from single-point cloud data. Meanwhile, Mohammadi et al. [18], Xu et al. [19] and Yang et al. [20] applied terrestrial LiDAR to look into how composite arch structures behave under sustained loads, paying particular attention to the masonry arch's bottom surface model where it meets the reinforced concrete supports.

There have been some attempts to use LiDAR for measuring structural displacements [21–25]. For instance, one study used a long-range, high-precision LiDAR that could measure displacements within a range of 3 to 5 mm [21]. But the downside is that using LiDAR often involves lengthy scanning times and adjustments, which can limit its usefulness for measuring dynamic displacements.

With advancements in Unmanned Aerial Vehicle (UAV), LiDAR, and visual tech,

new opportunities are available for bridge safety. While UAV inspections can help, they still need manual checks, which can lead to missed problems. Furthermore, there's no solid system right now for collecting and analyzing monitoring data, which also makes it hard to predict future issues based on provided data [26].

Langhammer and colleagues [27] developed a 3D model of a reservoir aimed at managing water and planning for flood control. They combined UAV with LiDAR technology, finding that LiDAR gave a more accurate estimate of the basin's volume. In another study, Li et al. [28] looked at two UAV-based systems—photogrammetry, and UAV and LiDAR—raw point cloud does a better job of capturing variations in the landforms compared to photogrammetry. Meanwhile, Rogers et al. [29] pointed out how effective LiDAR is for mapping vegetation, especially when used on UAV platforms.

Recent improvements in 3D reconstruction using artificial intelligence (AI) algorithms [30–34] have really opened doors for using them in displacement monitoring [35–37] via LiDAR combined with AI algorithms. With point cloud maps taken by Terrestrial LiDAR or LiDAR fixed on UAV, it can track structural displacement by comparing these point clouds of structural surfaces from different times using suitable AI algorithms. This is a novel and effective way to the best of the author's knowledge to monitor displacements in retaining structures, addressing the limitations and challenges that Terrestrial LiDAR or LiDAR fixed on UAV often face as mentioned in literature.

This paper is set to introduce a new approach combining LiDAR scanning technology and deep neural networks for inspecting hidden damage in bridges. The main goal is to enhance how we visualize and make decisions about maintenance along highways, decrease the need for manual inspection, and improve resource allocation and safety ratings on roadways.

2. Methodology

LiDAR-based structural assessments have definitely gained more interest in the structural health monitoring (SHM) field over the past few decades. However, there are still some challenges when it comes to the non-contact sensing method. One of the difficult parts of using LiDAR for monitoring is getting a high-quality, dense and uniform. If there are errors in the point cloud, it can lead to extra data or gaps, which negatively affect the ability of algorithms to detect any structural damage. The quality of the data collected by a LiDAR scanner depends on several factors, such as: (1) occlusions or extra objects in the way, (2) the properties of the surfaces being scanned, (3) how the scanner is positioned, (4) the specs of the scanner itself, and (5) the conditions of the environment. One of the biggest obstacles to obtaining a usable point cloud for structural analysis is dealing with all this excess data that needs to be sorted. Furthermore, it can get in the way, making it difficult to gather data on the actual things that matter.

This research begins by studying the actual needs for inspecting and maintaining private bridges. Using LiDAR scanning units (Terrestrial LiDAR and movable units fixed on UAV) integrated with a novel deep neural network (DNN) for structural monitoring of bridges based on the 3D mapping of bridge displacement compiled

from LiDAR scanning over time. The RNN-LSTM is selected to analyze the LiDAR point cloud maps, since the LiDAR scanning datasets have a time-dependent and memory-dependent behavior. The displacement value will be calculated by comparing these point clouds of bridge surfaces from different times using a suitable RNN-LSTM by searching for the node where the deformation occurred. The proposed displacement estimation technique response achieved a high accuracy rate, regression rate, and F-score. So, the data from LiDAR and DNN models can be combined to analyze the monitoring of transportation infrastructure. **Figure 1** illustrates the proposed displacement estimation technique.

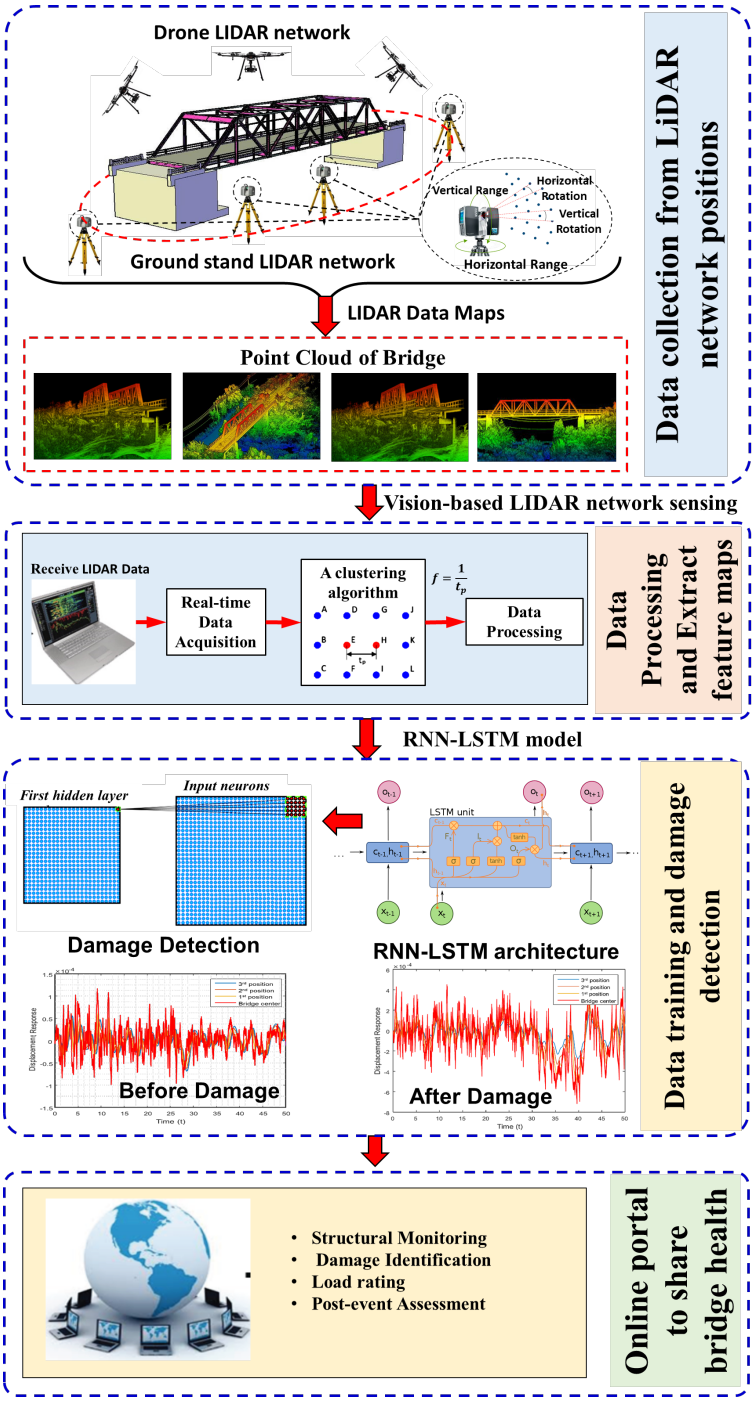

Figure 1. Schematic diagram of the proposed monitoring technique of the bridge.

2.1. Vehicle load classification

Collecting real-time data on passing vehicles is very difficult. We're talking about things like weight, type, spacing, and speed. So, first, its need to sort all the vehicles by weight or type. Then, figure out the key traits for different vehicle types, like axle load, wheelbase, track, and the maximum speed for each vehicle type.

On highways, there are tons of different vehicles, and transportation departments have their own ways of classifying them. Given the kind of traffic and the goals of this study, we really need to sort these vehicles and look closely at each group. Usually, highway agencies divide the vehicles into two main types: passenger cars and trucks. Then, each of those categories gets more specific based on how much they can carry, with about five subcategories. We can see the details in **Table 1**.

Table 1. Vehicle classification standards of the highway management department.

Type	Car (seat)	Truck (ton)
Type 1	≤7	≤2
Type 2	8–19	2–5
Type 3	20–39	5–10
Type 4	≥40	10–15
Type 5	no	>15

2.2. LiDAR technology

LiDAR tech is effective because it uses remote sensing to get good captures of the Earth's surface. Basically, it helps to check out what happened down there and collect all data in detailed geographical info. With LiDAR, you can create high-quality 3D digital models that show everything really well. The data results in a point cloud map, which is beneficial for mapping out whole cities. This way, decision-makers can identify structures and important areas with high accuracy, down to the millimeter level, see **Figure 2** for an example. Furthermore, the LiDAR can be used to identify and extract details about infrastructure like roads, bridges, tunnels, and even vegetation. Furthermore, it helps detect problems like surface wear or changes in the slope.

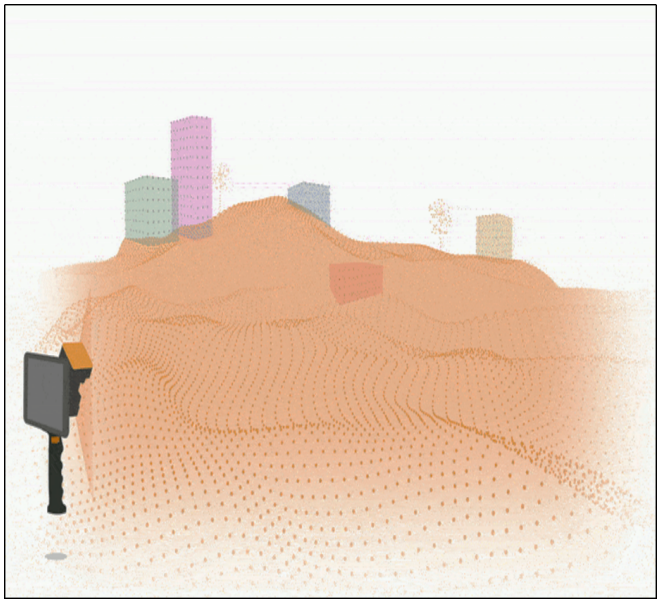

Figure 2. The LiDAR scanning fundamentals.

In bridges, the 3D LiDAR scanning is one of the effective monitoring technologies. First, it can give a highly accurate assessment of bridges that the usual inspection methods miss. Furthermore, it's automated, which means even a person without an experienced background can use it, it's perfect for the bridge inspectors. So it can set up the assessment rules easily. LiDAR is a neat digital tool that creates 3D maps of structures by collecting all various of coordinate data. It helps to detect things such as settling issues, cracks, and corrosion. Also, it decreases the risks and can speed up construction compared to traditional inspection methods, and it can collect the data anytime—day or night—on any structure.

3D LiDAR scanning abilities for bridge monitoring

Detecting and measuring issues with bridge structures can really help detect any stability concerns. It can use point cloud maps from LiDAR scans to easily find physical damage on bridges. With some easy algorithms, data about things like surface wear or concrete loss from vehicle collisions can be extracted. **Figure 3a** shows how can see that it's easy to estimate visible damage using the surface data from LiDAR scans. **Figure 3b** shows how to get accurate vertical clearance data, with millimeter precision using the LiDAR data. **Figure 3c** shows how we found four damaged areas on two out of the four beams we scanned, and measured the mass loss and volume for each damaged area. Finally, **Figure 3d** displays the load-deflection measurements at different points using the 3D LiDAR scanner, showing how deflection is clear for position 1 when a truck is loaded.

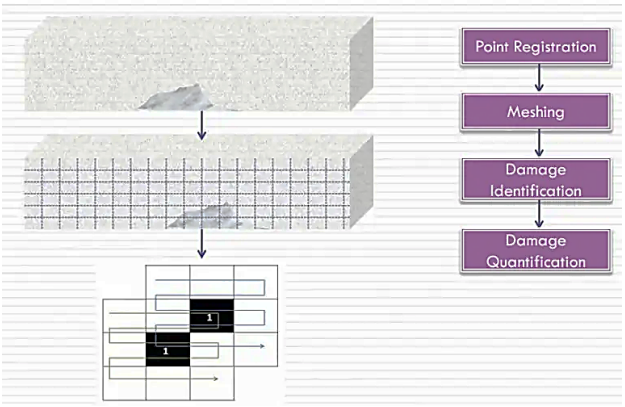

(a) Estimate a visible damage.

(b) Get a vertical clearance.

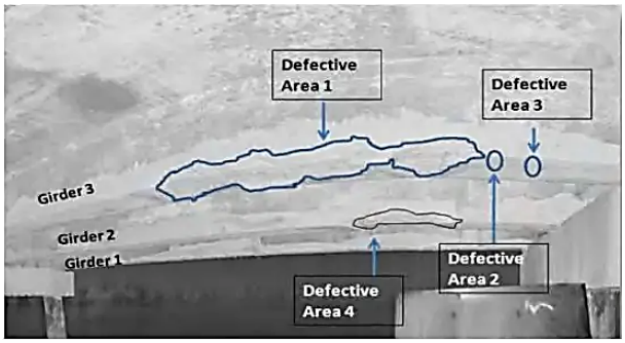

No.	Area (m^2)	Volume (m^3)
1	0.507	0.0285
2	6.62×10^{-4}	2.63×10^{-5}
3	2.13×10^{-4}	7.11×10^{-6}
4	0.225	0.0156

(c) Measured the mass loss and volume of the damage area.

Figure 3. *Cont.*

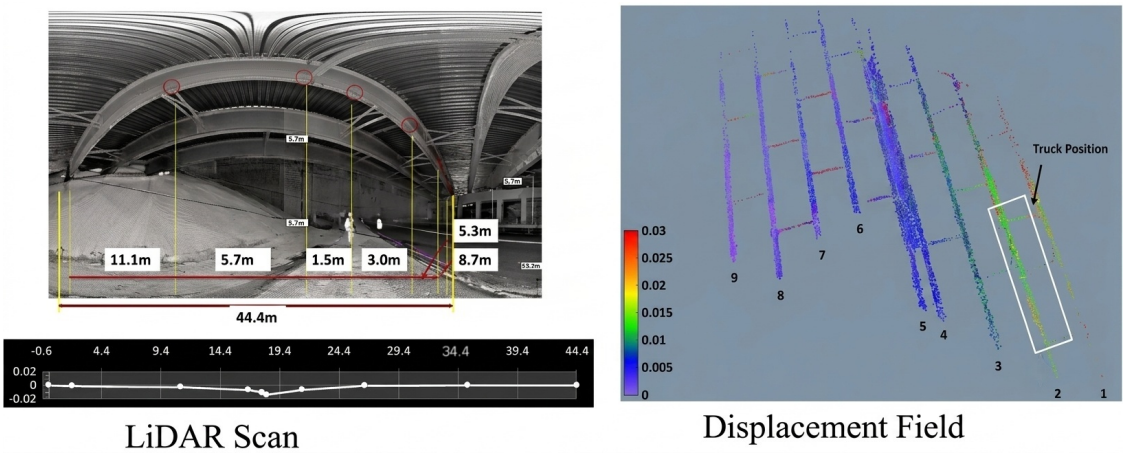

(d) The load-deflection measurements.

Figure 3. 3D LiDAR Scanning Abilities for Bridges Monitoring [37].

2.3. RNN-LSTM configuration

In this study, we opted for the RNN-LSTM model over a traditional feedforward neural network to monitor bridge damage. This choice makes sense because the datasets from LiDAR sensors are both time-dependent and memory-dependent. The LSTM helps address the issue where the error signal used for training the network tends to diminish exponentially as we go further back in time within the RNN, illustrated in **Figure 4**. This figure outlines the deep learning model we proposed to describe the restoring force in the hysteretic structural system of the bridge. Here, the input consists of the LiDAR sensor datasets, while the output focuses on detecting and classifying bridge damage [38].

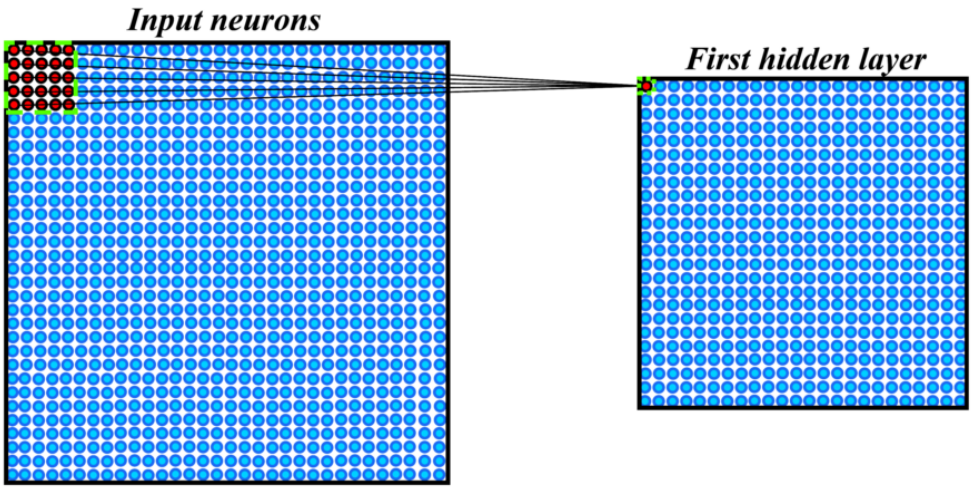

Figure 4. Structure of the LSTM cell and weight connections [38].

At each moment in a time series, an LSTM cell monitors a hidden vector and a memory vector, which help it manage its updates and outputs effectively. The output or activation for each LSTM cell is defined as follows:

$$h_t = \Gamma_o . \tanh(C_t) \tag{1}$$

where Γ_o is the output gate that controls the amount of information shared from memory

(C_t), and here's how it's calculated:

$$\Gamma_o = \sigma(W_o.[h_{t-1}, X_t] + b_o). \tag{2}$$

So here's the deal: at any given time step (t), we have the input for the LSTM (X_t) and we're using the sigmoid activation function (σ). There's this weight matrix (W_o) that controls how the output gate operates. Then we've got h_{t-1}, which is the activation or hidden vector from the previous time step ($t-1$) taken from the last LSTM cell. Plus, there's a bias (b_o) that comes into play when we're figuring out the output.

Now, C_t represents the memory cell or vector that helps forget some of what's currently stored (C_{t-1}), pulls from the previous LSTM cell, and takes in new memory content ($\widehat{C}_t$). We can define that as follows:

$$C_t = \Gamma_f.C_{t-1} + \Gamma_u.\widehat{C}_t. \tag{3}$$

Here's how the content of the new memory ($\widehat{C}_t$) gets updated:

$$\widehat{C}_t = \tanh\left(W_c.[h_{t-1}, X_t] + b_c\right). \tag{4}$$

So we have this weight matrix, W_c, and it pretty much controls how our new memory operates. Then there's the bias, b_c, which plays a role in shaping that memory.

In Equation (3), we introduce Γ_f, which helps figure out how much of the current memory we need to forget, hence the name forget gate. Then there's Γ_u, another part that manages how much new info we actually add to the memory cell, which we refer to as the update/input gate. Since these gates are in charge of what's stored in memory, their values have to stay between zero and one. We accomplish that by using the sigmoid function in their setup. The next calculations will show us how that works.

$$\Gamma_f = \sigma(W_f.[h_{t-1}, X_t] + b_f) \tag{5}$$

$$\Gamma_u = \sigma(W_u.[h_{t-1}, X_t] + b_u) \tag{6}$$

In this configuration, W_f and W_u are the weight matrices that control how the forget gate and the input/update gate operate. Essentially, h_t and C_t are the outputs from the LSTM cell at time step *t*, which get sent to the next cell at time step $t+1$. If the LSTM cell at time step t generates this output, here's how we can calculate it:

$$O_t = \text{softmax}(W_o.h_t + b_o). \tag{7}$$

Figure 5 illustrates the structure of the LSTM cell.

2.3.1. Bidirectional LSTM

Bidirectional architecture is essentially a flexible framework that can be integrated with any RNN model, LSTM included. In a biLSTM (or bidirectional LSTM) cell, we'll find two standard unidirectional LSTM cells working together: one analyzes past time steps and the other looks at future ones. **Figure 6** gives us a picture of how a biLSTM cell is structured.

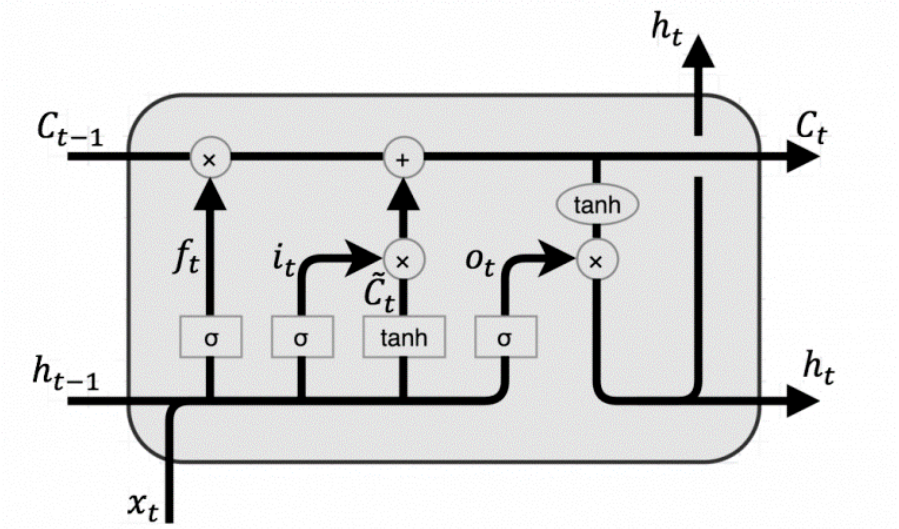

Figure 5. A single block diagram in an RNN-LSTM [39].

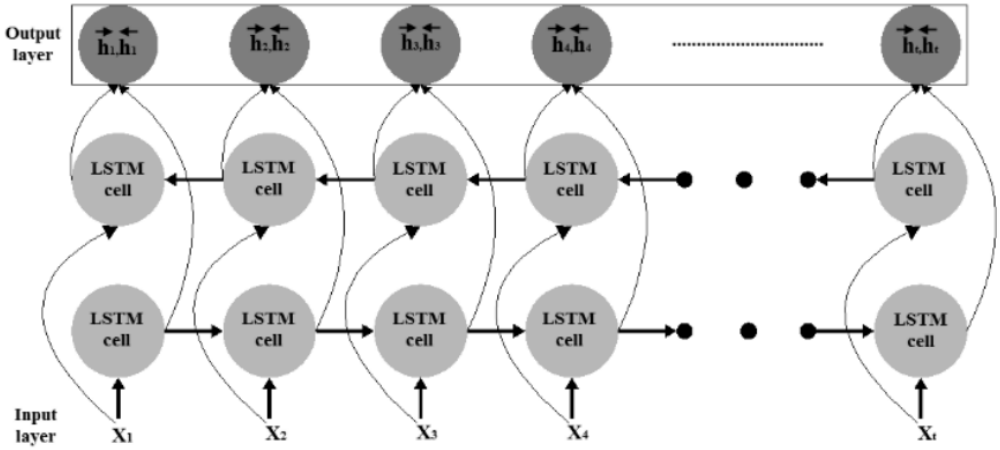

Figure 6. The biLSTM structure.

At each time step, the biLSTM keeps track of two hidden states—one for the past and another for the future. This feature really boosts its performance for sequence-related tasks, like text classification. Speaking of that, we've categorized structural damage detection as a sequence classification problem in this study [40].

So, if a biLSTM cell generates an output at a particular time step, here's how we can compute it:

$$O_t = \text{softmax}(W_o.[\overrightarrow{h}_t, \overleftarrow{h}_t] + b_o) \tag{8}$$

here, $\overrightarrow{h}_t$ and $\overleftarrow{h}_t$ refer to the activations of the forward and backward biLSTM cells at time step t.

2.3.2. Bayesian genetic algorithms

There are several ways to make Bayesian genetic algorithms (BGA) work better for objective functions (f), like using Gaussian processes [41–43], random forests [44], and tree-structured Parzen estimators [45, 46]. If we check out **Figure 7**, we'll see a comparison of the Grid search, Random search, and BGA optimization methods for tuning the model's hyperparameters. The numbered circles show how well the model did using each method. It's interesting to note that while the Grid search covers

broader areas, BGA optimization techniques can explore different combinations more intelligently and often find the best solutions with fewer tests. For this study, we decided to go with BGA techniques to speed up and enhance training.

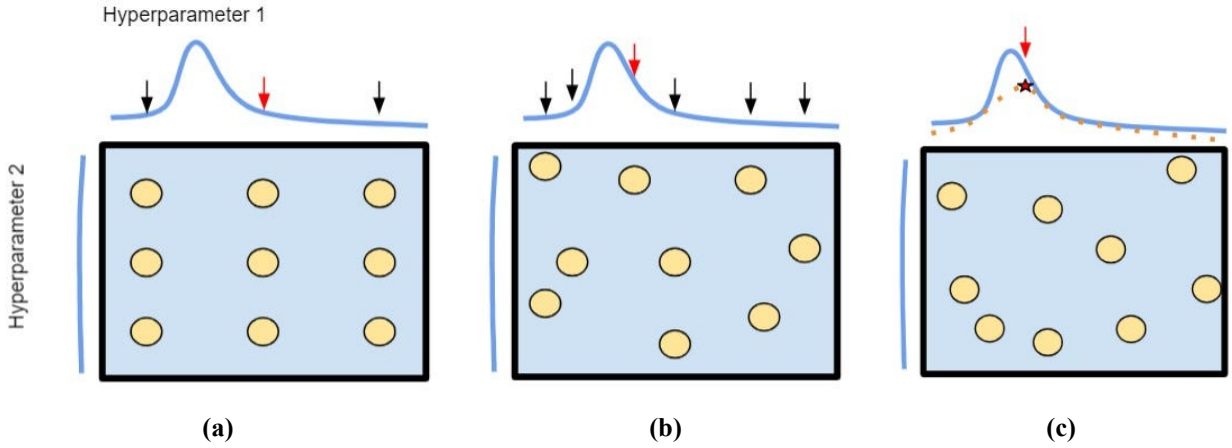

Figure 7. The comparison between **(a)** grid search vs. **(b)** random search. vs. **(c)** BGA optimization techniques for tuning the model's hyperparameters.

3. Case study

3.1. Bridge overview

Figure 8 presents the Huangshan River Bridge in the Zhuji section, Huangshan City, China. The Bridge has 439.52 m length, 12 m width, and 14 × 30 m for bridge upper structure of simply supported prestressed concrete composite box beams. The lower part of the bridge is U-shaped and adopts pile-type piers. The design load of the bridge is 20 t for cars and 120 t for trailers.

Figure 8. Huangshan River Bridge.

3.2. Bridge test via LiDAR

In this study, we performed a group of Terrestrial LiDAR units fixed on holders and movable units fixed on UAVs in shooting places to apply the field test on bridges in common use for structural monitoring in places where the visual inspection is impossible beyond human control and verify the reliability of the proposed method as shown in **Figure 9**.

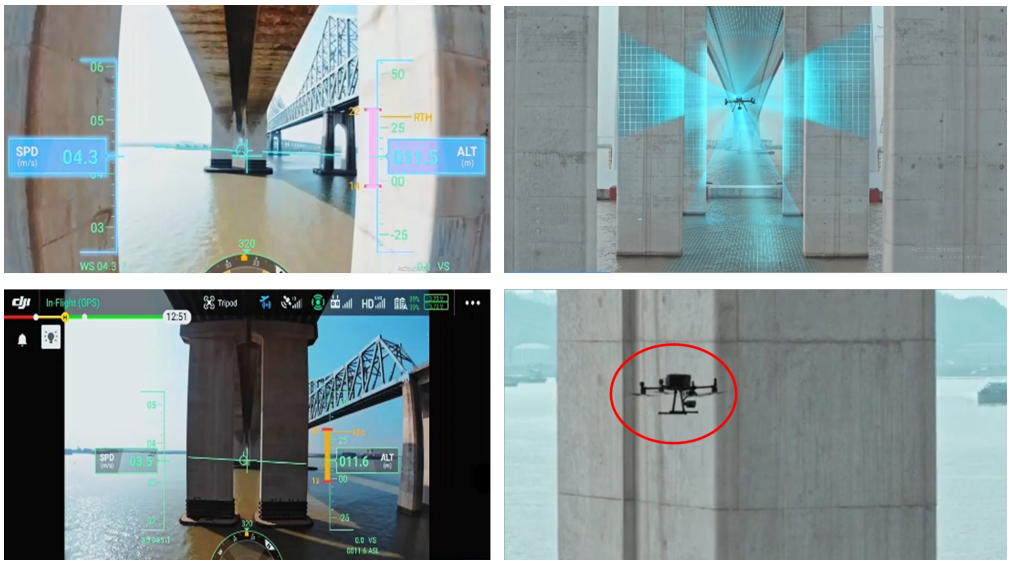

Figure 9. Image acquisition from UAV and LiDAR.

3.3. Feature extraction

The setup features an RNN-LSTM that starts with an input layer for the LiDAR point cloud maps of the bridge, incorporating the mode shapes of the bridge. This is followed by three 1D convolutional layers designed to eliminate data outliers (**Figure 10**), each with its own configurations: the first layer is set to 56 × 128, the second to 28 × 256, and the third to 14 × 512. Then, we include two sub-sampling LSTM layers, sized at 14 × 512 and 7 × 512. Afterward, we flatten all the 2D arrays from the pooled feature maps into a single long vector containing 25,088 elements. The output layer uses a softmax activation function to predict the bridge displacement. It's also important to note that while both the RNN and CNN models share similar architectures, they differ in the feature extraction areas near the input layer. We evaluate both the cost and accuracy of these models, checking the test set accuracy before and after training. To speed up training and improve accuracy, we used the BGA technique.

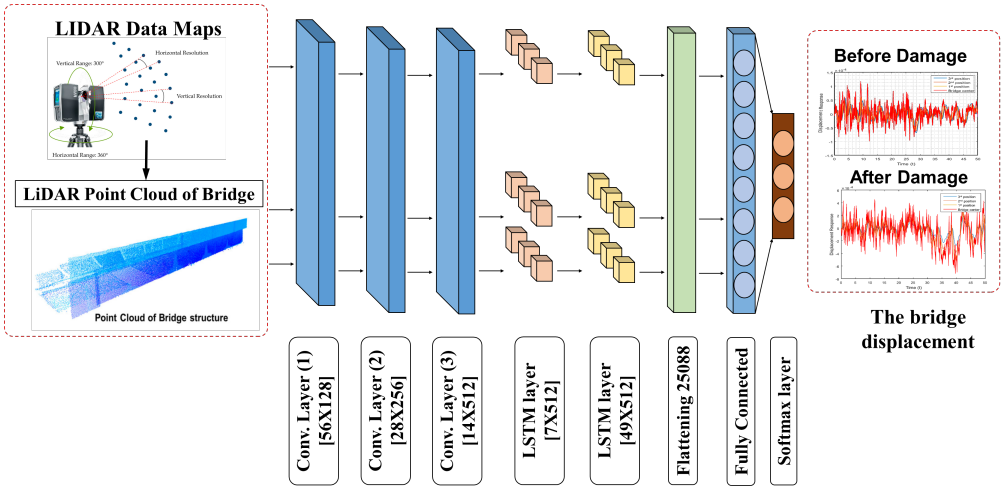

Figure 10. The deep learning network includes three 1-D convolutional layers, full connection layers, two sub-sampling LSTM layers, and a softmax layer.

Extracting related functions is the main task of creating a global map, and it can be easy to perform localized tasks by providing the environment and shapes

around the environment of environmental or bridge load. **Figure 11** shows a simple workflow architecture, including training the load locations and feature extraction. In this part of the study, we must analyze the method of solving the localization and mapping problems of bridge displacement, and these problems can be expanded to other autonomous systems. Our method is only based on LiDAR measurements to locate the load. We assume that the LiDAR scanning and ground real locations are in the body frame, and each location has a corresponding scan at each time stamp. We use non-semantic functions to distinguish some related prototypes. Compared with a single object (such as a pole or edge), this technology can detect various objects in the environment, which is very beneficial to the environment with less texture data. We choose to use a cluster algorithm to extract clusters, which constitute our non-semantic characteristics.

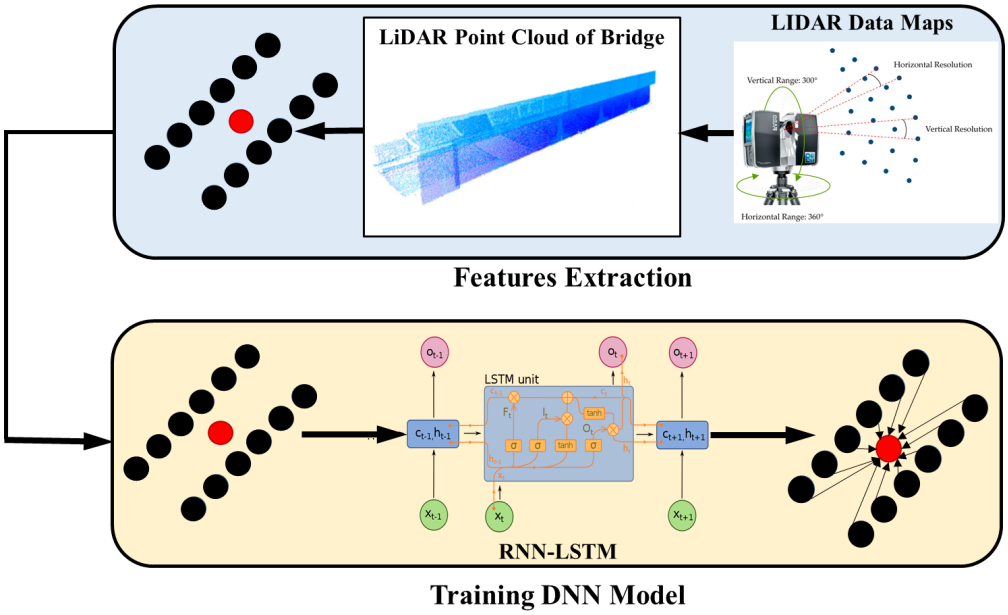

Figure 11. Workflow architecture diagram.
Note: Features are extracted from LiDAR scans (black dots) and an RNN-LSTM is trained to estimate the real position of damages (red dot).

Let P_t be a LiDAR scanning at time t:

$$P_t = \{p_{t,i}\}_{i\in[1,\ D_t]} \tag{9}$$

where $p_{t,i} = [x_i,\ y_i,\ z_i]$, D_t is the points number of LiDAR at time t, and $S_t = [s_{t,\ i},\ s_{t,j}]$ is the actual position at time t. We apply a clustering method to fix the centers number to a certain value:

$$C_t = \{c_{t,i}\}_{i\in[1,\ \acute{D}_t]} \tag{10}$$

Where $c_{t,i} = [\acute{x}_i,\ \acute{y}_i,\ \acute{z}_i]$, $\acute{D}_t$ is the clusters number, C_t is the centers group of the clusters and $c_{t,i}$ is the center point of the cluster i, where $i \in \left[1,\ \acute{D}_t\right]$. For simplicity in the following we assume that the number of clusters remains constant along the trajectory ($\acute{D} = \acute{D}_t$ for all t).

As the target of this work is to find the bridge displacement $\left[\alpha_{t,1}, \alpha_{t,2}, \ldots\ldots, \alpha_{t,\acute{D}_t}\right]$ that will minimize the position(p) using objective function $f\left((w_{t,i}, c_{t,i}, \alpha_{t,i}) - S_t\right)$ at time $t = 1, \ldots T$ with constraints $w_{t,1}, w_{t,2}, \ldots w_{t,\acute{D}_t} \in R^+$, $\alpha_{t,1}, \alpha_{t,2}, \ldots, \alpha_{t,\acute{D}_t} \in R^+$. Where T is the last timestamp value, $w_{t,i}$ are some weights at the measuring cluster.

In order to estimate the bridge displacement at various positions efficiently and at low cost to avoid the huge and complicated mathematical processes above, we established a new technique using a novel DNN based on RNN-LSTM, which feeds the cluster features at time t and various positions as input, and the estimated displacement of each position of the bridge is returned, as shown in **Figure 1**.

3.4. Training, validation, and test sets

In this research, we selected the mean square error (MSE) for optimizing the network parameters such as the weights and bias in the layers. The training mode uses the cluster features at time t and various positions to adjust the network parameters for controlling the hidden layer numbers that change due to the training mode results. We obtain satisfactory results at the output of the network after several iterations of testing. The training ends when the MSE becomes a steady state at the low value of MSE. The RNN-LSTM setup, training, and testing model functions are presented in **Figure 12**. The training performance of the suggested DNN is presented in **Figure 13** where an Epoch refers to one cycle through the full training dataset. The training key parameters are presented in **Table 2**. The steps of the MATLAB code of RNN training and evaluating are presented in **Algorithm 1**.

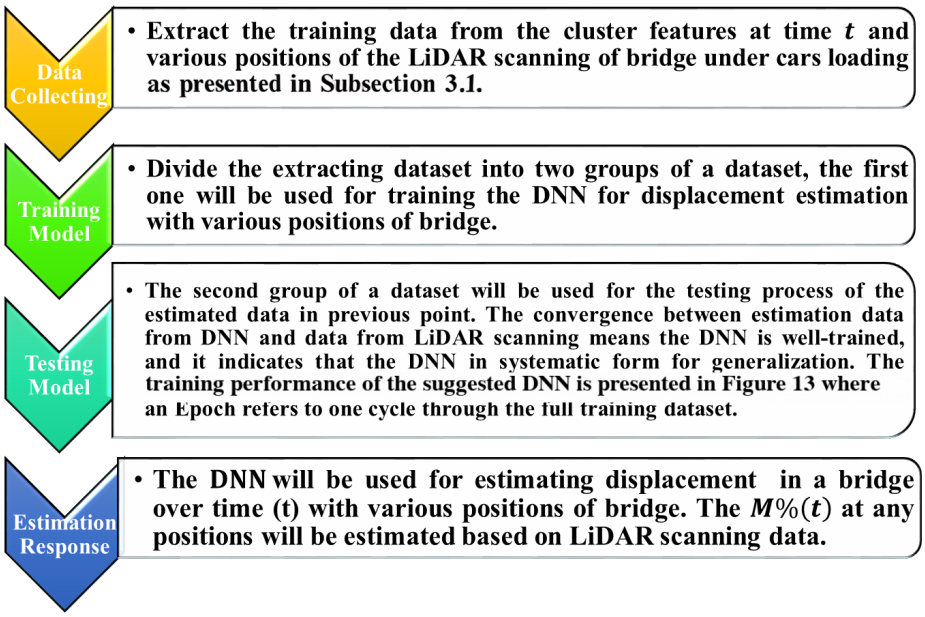

Figure 12. The steps of DNN training to estimate the bridge displacement.

Table 2. RNN key parameters.

Training time	Gauge	Training rate	Attenuation factor
75 s	36	10^{-4}	10^{-6}

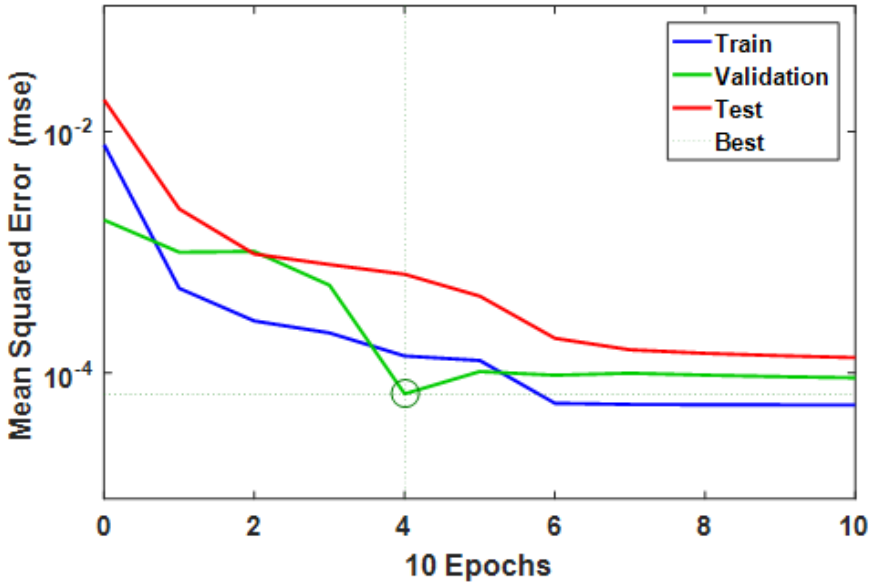

Figure 13. RNN Training Performance.

Algorithm 1 Training and evaluating the RNN

algorithm RNN
input: P: $p_{t,i}$ dataset, t: time, $c_{t,i}$ dataset, $w_{t,i}$, S_t W: Network parameter matrix weight w_{ij} and bias b_j
output: score of DNN trained model on the dataset to estimate bridge displacement $\alpha_{t,i}$ for various ε, EPD
let f be the feature set 3d matrix
for *i* in the dataset **do**
  let f_i be the feature set matrix of sample l
  for *j* in *i* **do**
    $V_i \leftarrow vectorize_{(j,w)}$
    append V_i to f_i
    append f_i to f
  $f_{train}, f_{test}, l_{train}, l_{test}$ ← the split feature set and prediction into train subset and test subset
  $M \leftarrow DNN\ (f_{train}, l_{train})$
  score ← evaluation (l, l_{test}, M)
  return score
end for
end for

4. Results and discussions

4.1. Displacement analysis

To measure displacement using LiDAR data, first we collected the point cloud data at different time points as shown in Section 3.3, then compared the point clouds to identify changes in the positions of specific points or features, allowing for the calculation of displacement.

1. Point-to-Point: Compare the coordinates of corresponding points in the aligned point clouds to determine the displacement vector.
2. Surface-Based: Compare the surfaces of the point clouds to identify changes in shape or position.
3. Grid-Based: Create a grid on the point cloud and compare the displacement of grid points.
4. Triangle Grid-Based: displacement is calculated using three points on the same

line.

5. Least Squares-Based: Calculate the distance to each point by selecting a random line.

Laser scanning was performed at four positions on the bridge with each load case lasting 50 s, and a total of 40 scans were obtained (including no-load conditions). The displacement evaluation technique is based on the bridge point cloud data. The maximum displacement occurs at 219.76 m in the center of the bridge, and the displacement results are presented in **Figures 14** and **15** before and after bridge damage occurred respectively, where the 1st position at 109.88 m from the bridge center, the 2nd position at 164.82 m from the bridge center, and the 3rd position at 192.29 m from the bridge center.

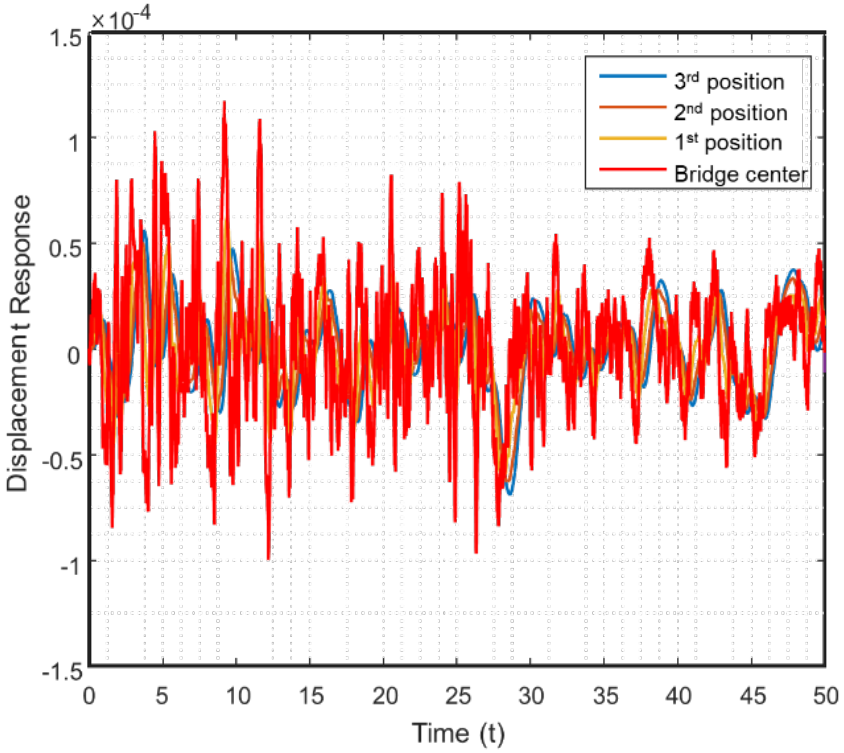

Figure 14. The bridge displacement before damages, where the 1st position at 109.88 m, 2nd position at 164.82 m, and 3rd position at 192.29 m from the bridge center.
Note: A scale factor of 10^{-4} is applied to the y-axis, as indicated at the top of the axis.

4.2. Proposed method accuracy and reliability evaluation

We look at four main things to check how well the proposed method is doing: the false negative rate (FNR), false positive rate (FPR), true negative rate (TNR), and true positive rate (TPR). Here's how we can tweak the performance based on those:

$$\text{accuracy rate } (P\%) = \frac{N_{TPR}}{N_{TPR} + N_{FPR}} \tag{11}$$

$$\text{regression rate } (R\%) = \frac{N_{TPR}}{N_{TPR} + N_{FNR}} \tag{12}$$

$$\text{F score } (F\%) = \frac{2N_{TPR}}{2N_{TPR} + N_{FNR} + N_{FPR}} \tag{13}$$

In this research, we prepared 40 datasets from LiDAR measurement to test things out, splitting them into 8 groups based on the output displacement in the pavement to get results for g_1, g_2 and so on up to g_8. This all happened after running a thousand iterations, or epochs, to check if the CNN really works. Overall, the performance metrics were very good, with $P\%$ at 96.43%, $R\%$ at 93.77%, and $F\%$ at 91.65%. So, it looks like this method can accurately detect displacement in the pavement. **Figure 16** shows how those $P\%$, $R\%$, and $F\%$ values changed over those $1,000$ Epochs.

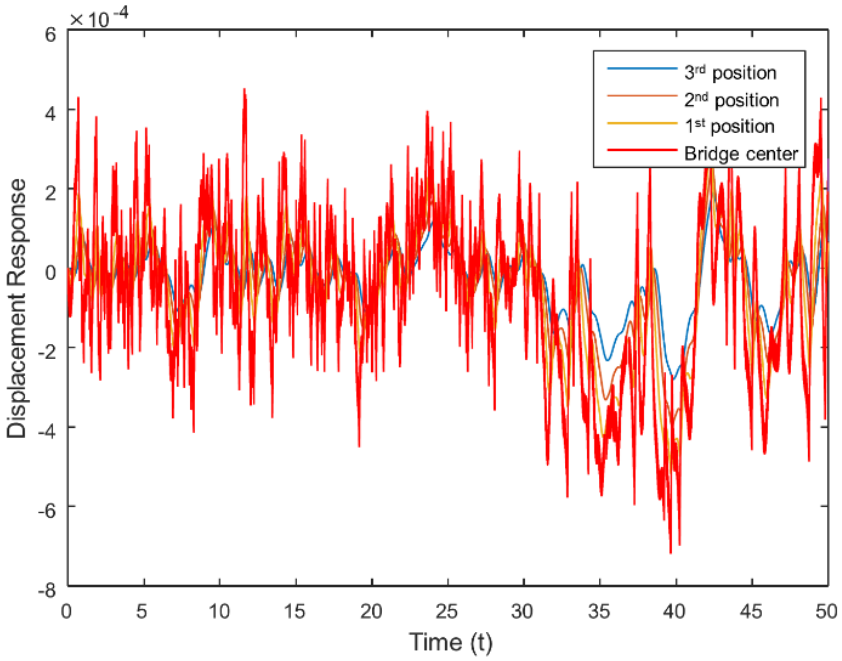

Figure 15. The bridge displacement after damage, where the 1st position is at 109.88 m, the 2nd position at 164.82 m, and the 3rd position at 192.29 m from the bridge center.
Note: A scale factor of 10^{-4} is applied to the y-axis, as indicated at the top of the axis.

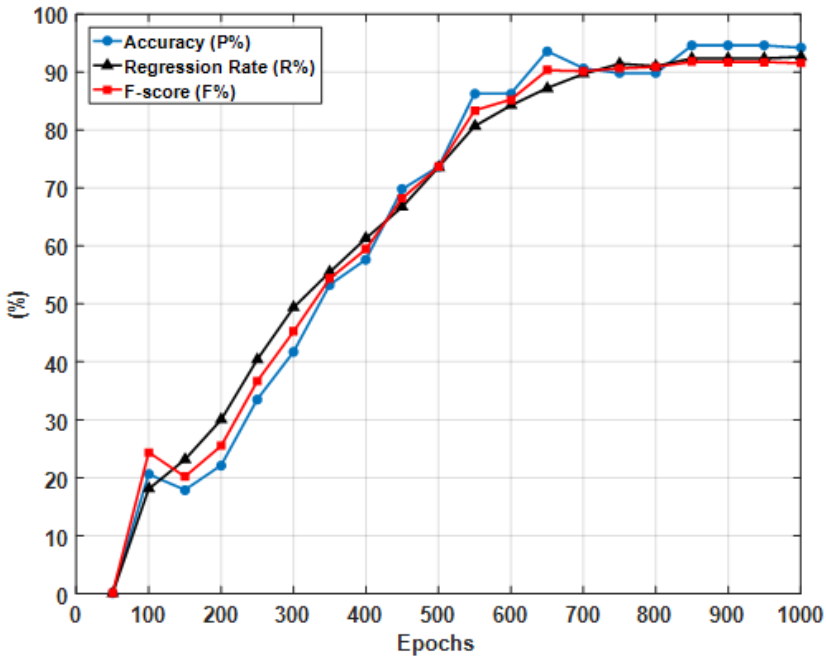

Figure 16. The training proceeded with a comparison based on the displacement in the bridge.

To improve the experimental section of a deep learning study, we compared the performance of the proposed model (RNN-LSTM based on a LiDAR response) against two other traditional methods (contact technique) to estimate the bridge displacement in literature such as CNN based fiber optic sensors response by Sun et al. [47], and ANN based strain gauge and accelerometer response by Ma et al. [48]. This contextualizes the model's efficacy and demonstrates its advantage over existing methods. The results of multiple models are often compared using a confusion matrix and a side-by-side look at baselines and proposed models highlight how well the model can tell apart bridge displacement estimation.

The confusion matrix is presented in **Figure 17**. It outlines how effectively each model for bridge displacement estimation for the RNN-LSTM is based on a LiDAR response. The confusion matrix is plotted for algorithms that have better F1-score values. Just so we know, any values below 1% are considered zero in these matrices. **Figure 17** indicates that the RNN-LSTM based a LiDAR response is performing quite well, showing higher average accuracy and appearing to have the advantage over other contact techniques. Average accuracies are 89.42%, and 92.46%, for the ANN and CNN respectively.

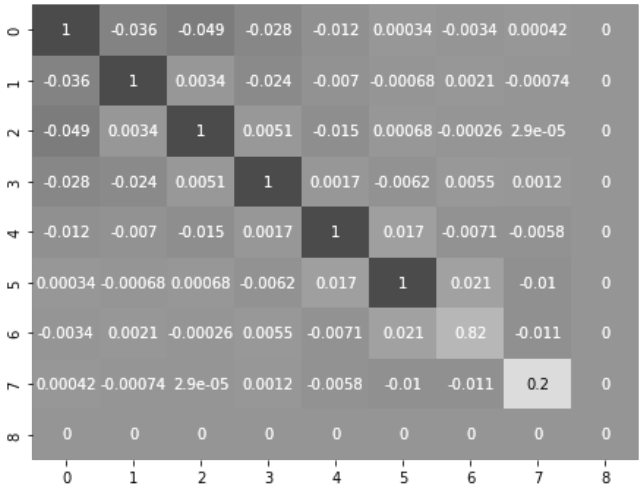

(a) RNN-LSTM based a LiDAR response.

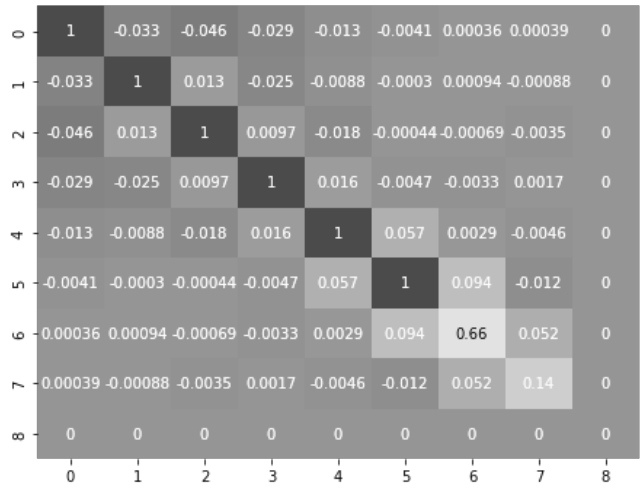

(b) CNN based fiber optic sensors' response.

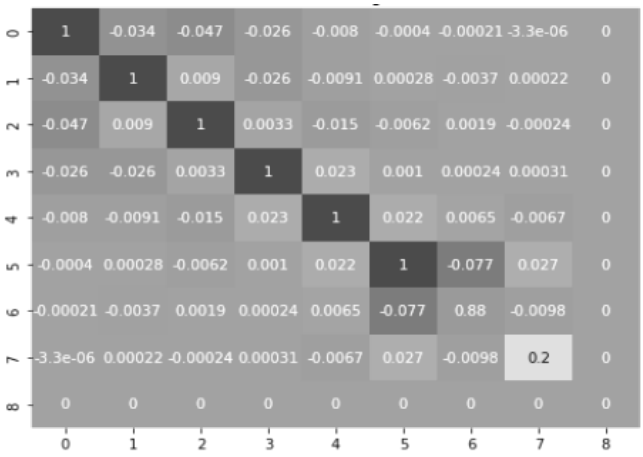

(c) ANN based strain gauge and accelerometer response.

Figure 17. The confusion matrices for the RNN-LSTM and other algorithms used in the literature.

5. Conclusion

In this work, the LiDAR scanning units (Terrestrial LiDAR fixed on holders and movable units fixed on UAV) were integrated with a novel deep neural network (DNN) for damage monitoring of bridges. Considering the analysis conducted in this study, the monitoring model is based on the RNN-LSTM platform since the LiDAR scanning datasets are a time time-dependent and memory-dependent. The displacement estimation technique was applied using the point cloud of the bridge at four positions on the bridge (1st position at 109.88 m from the bridge center, the 2nd position at 164.82 m from the bridge center, and the 3rd position at 192.29 m from the bridge center) for 50 s for each load case that was collected for training the DNN, and we found that the maximum displacement occurs at the center of the bridge at 219.76 m before and after bridge damages occurred. It has been found that the response of the proposed DNN achieved high rates of P%, R%, and F% equal to 96.43%, 93.77%, and 91.65% respectively. It stands out in the confusion matrix analysis, plus a LiDAR response (non-contact technique) of bridge displacement predicted and actual conditions against two other traditional methods (contact technique) to estimate the bridge displacement in literature such CNN based fiber optic sensors response, and ANN based strain gauge and accelerometer response, highlights the distinguish the model between the different levels of bridge displacement estimation. So, the data from LiDAR and DNN models can be combined to analyze the monitoring of transportation infrastructure.

Funding: This research received no external funding.

Institutional review board statement: Not applicable.

Informed consent statement: Not applicable.

Data availability statement: Not applicable.

Conflict of interest: The author declares no conflict of interest.

AI use statement: The author declares that no artificial intelligence (AI) tools were used in the preparation of this manuscript.

References

1. Altabey WA, Noori M, Wu Z. Deep Learning-Based Crack, Location and Area Identification for a Pipeline by The Convolutional Neural Network Based on Crack Contour Network Method. In: Proceedings of the 9th International Conference on Computational Methods in Structural Dynamics and Earthquake Engineering; 12–14 June 2023; Athens, Greece. doi: 10.7712/120123.10644.20187
2. Altabey WA. The Advanced Structural Health Monitoring by Non-Destructive Self-Powered Wireless Lightweight Sensor. Structural Durability & Health Monitoring. 2025; 19(6): 1529–1545. doi: 10.32604/sdhm.2025.069003
3. Altabey WA. An Intelligent System for Pavement Health Monitoring Using Perception Sensors Aided Deep Learning Algorithms. Structural Durability & Health Monitoring. 2026; 20(2): 5. doi: 10.32604/sdhm.2025.073949
4. Altabey WA, Noori M, Wu Z, et al. Effective Technique for Structures Damage Detection Based on the Structural Frequency Maps. In: Proceedings of the 9th International Conference on Computational Methods in Structural Dynamics and Earthquake Engineering; 12–14 June 2023; Athens, Greece. doi: 10.7712/120123.10645.21865
5. Ma Z, Choi J, Sohn H. Structural displacement sensing techniques for civil infrastructure: A review. Journal of

Infrastructure Intelligence and Resilience. 2023; 2(3): 100041. doi: 10.1016/j.iintel.2023.100041
6. Bunce A, Hester D, Taylor S, et al. A robust approach to calculating bridge displacements from unfiltered accelerations for highway and railway bridges. Mechanical Systems and Signal Processing. 2023; 200: 110554. doi: 10.1016/j.ymssp.2023.110554
7. Xiao X, Han H, Wang J, et al. Dynamic Deformation Analysis of Super High-Rise Buildings Based on GNSS and Accelerometer Fusion. Sensors. 2025; 25(9): 2659. doi: 10.3390/s25092659
8. Hou S, Zeng C, Zhang H, et al. Monitoring interstory drift in buildings under seismic loading using MEMS inclinometers. Construction and Building Materials. 2018; 185: 453–467. doi: 10.1016/j.conbuildmat.2018.07.087
9. Tamura Y, Matsui M, Pagnini LC, et al. Measurement of wind-induced response of buildings using RTK-GPS. Journal of Wind Engineering and Industrial Aerodynamics. 2002; 90: 1783–1793. doi: 10.1016/S0167-6105(02)00287-8
10. Shen N, Chen L, Liu J, et al. A review of global navigation satellite system (GNSS)-based dynamic monitoring technologies for structural health monitoring. Remote Sensing. 2019; 11(9): 1001. doi: 10.3390/rs11091001
11. Blais F. Review of 20 years of range sensor development. Journal of Electronic Imaging. 2004; 13: 231–243. doi: 10.1117/1.1631921
12. Ma Z, Lee J, Choi J, et al. Two-dimensional horizontal displacement estimation for building structures by fusing acceleration and sparse point clouds. Mechanical Systems and Signal Processing. 2025; 225: 112318. doi: 10.1016/j.ymssp.2025.112318
13. He S, Zhou Z, Chu X, et al. Bridge deck deformation analysis based on vehicle borne three-dimensional laser scanning results. Science Technology and Engineering. 2019; 19: 268–276. (in Chinese)
14. Tan D, Li W, Tao Y, et al. Bridge Deformation Monitoring Combining 3D Laser Scanning with Multi-Scale Algorithms. Sensors. 2025; 25(13): 3869. doi: 10.3390/s25133869
15. Artese S, De Ruggiero M, Taliano Grasso A, et al. The survey, the representation and the structural modeling of the S. Angelo roman bridge on the Savuto river (Scigliano, Calabria, Italy) for diagnostics and conservation aims. Journal of Physics: Conference Series. 2022; 2204(1): 012095. doi: 10.1088/1742-6596/2204/1/012095
16. Sedek M, Serwa A. Development of new system for detection of bridges construction defects using terrestrial laser remote sensing technology. The Egyptian Journal of Remote Sensing and Space Science. 2016; 19(2): 273–283.
17. Park HS, Lee HM, Adeli H, et al. A new approach for health monitoring of structures: Terrestrial laser scanning. Computer-Aided Civil and Infrastructure Engineering. 2007; 22(1): 19–30.
18. Mohammadi M, Rashidi M, Azandariani MG, et al. Modern damage measurement of structural elements: Experiment, terrestrial laser scanning, and numerical studies. Structures. 2023; 58: 105574. doi: 10.1016/j.istruc.2023.105574
19. Xu X, Yang H, Neumann I. Deformation monitoring of typical composite structures based on terrestrial laser scanning technology. Composite Structures. 2018; 202: 77–81.
20. Yang H, Xu X, Neumann I. Deformation behavior analysis of composite structures under monotonic loads based on terrestrial laser scanning technology. Composite Structures. 2018; 183: 594–599.
21. Tzortzinis G, Ai C, Breña SF, et al. Using 3D laser scanning for estimating the capacity of corroded steel bridge girders: Experiments, computations and analytical solutions. Engineering Structures. 2022; 265: 114407. doi: 10.1016/j.engstruct.2022.114407
22. Truong-Hong L, Laefer DF. Using Terrestrial Laser Scanning for Dynamic Bridge Deflection Measurement. Available online: http://hdl.handle.net/10197/7495 (accessed on 16 May 2024).
23. Kim K, Sohn H. Dynamic displacement estimation by fusing LDV and LiDAR measurements via smoothing based Kalman filtering. Mechanical Systems and Signal Processing. 2017; 82: 339–355. doi: 10.1016/j.ymssp.2016.05.027
24. Lee J, Lee KC, Lee S, et al. Long-Term Displacement Measurement of Bridges Using a LiDAR System. Ulsan National Institute of Science and Technology; 2019. (in Korean)
25. Lee J, Kim RE. Noncontact dynamic displacements measurements for structural identification using a multi-channel Lidar. Structural Control and Health Monitoring. 2022; 29: e3100.
26. Runqiu Z, Tinglin L, Hong W, et al. Machine vision approach of bridges crack identification based on the fusion of UAV vision and LiDAR. In: Proceedings of the 4th International Civil Engineering and Architecture Conference; 15–17 March 2024; Seoul, Republic of Korea. pp. 39–50. doi: 10.1007/978-981-97-5477-9_4
27. Langhammer J, Janský B, Kocum J, et al. 3-D reconstruction of an abandoned montane reservoir using

UAV photogrammetry, aerial LiDAR and field survey. Applied Geography. 2018; 98: 9–21. doi: 10.1016/j.apgeog.2018.07.001
28. Li T, Zhang B, Xiao W, et al. UAV-based photogrammetry and LiDAR for the characterization of ice morphology evolution. IEEE Journal of Selected Topics in Applied Earth Observations and Remote Sensing. 2020; 13: 4188–4199. doi: 10.1109/JSTARS.2020.3010069
29. Rogers SR, Manning I, Livingstone W. Comparing the spatial accuracy of digital surface models from four unoccupied aerial systems: photogrammetry versus LiDAR. Remote Sensing. 2020; 12(17): 2806. doi: 10.3390/rs12172806
30. Meng F, Qiao S, Chen D. A Data-Driven framework for precise geometric measurement of tunnel structures using 3D point clouds and Bayesian optimization. Measurement. 2026; 271: 120931. doi: 10.1016/j.measurement.2026.120931
31. Zou J, Li Y, Zhou Y, et al. Deformation Detection of the Centroid Axes for Beams with Variable Cross-Sections Based on Point Cloud Data. Applied Sciences. 2026; 16(4): 2008. doi: 10.3390/app16042008
32. Luo K, Guan T, Ju L, et al. P-MVSNet: Learning patch-wise matching confidence aggregation for multi-view stereo. In: Proceedings of the IEEE International Conference on Computer Vision; 27 October–2 November 2019; Seoul, Republic of Korea. doi: 10.1109/ICCV.2019.01055
33. Wang F, Galliani S, Vogel C, et al. PatchMatchNet: Learned multi-view patchmatch stereo. In: Proceedings of the IEEE Computer Society Conference on Computer Vision and Pattern Recognition; 20–25 June 2021; Nashville, TN, USA. doi: 10.1109/CVPR46437.2021.01397
34. Altabey WA. An Artificial Intelligence-Based Scheme for Structural Health Monitoring in CFRE Laminated Composite Plates under Spectrum Fatigue Loading. Structural Durability and Health Monitoring. 2025; 19(5): 1145–1165. doi: 10.32604/sdhm.2025.068922
35. Chu M, Ma X, Wang X, et al. Research on coaxiality error measurement methodology for rectangular spline shafts using 3D point cloud technology. Measurement Science and Technology. 2025; 36(12): 125010. doi: 10.1088/1361-6501/ae1f2f
36. Feng Y, Feng SJ, Zhang XL, et al. Automatic deformation detection of metro tunnels via point cloud segmentation and geometric analysis. Automation in Construction. 2026; 181: 106657. doi: 10.1016/j.autcon.2025.106657
37. Gis Resources. LiDAR Technology for Monitoring Bridge Structure Defect and Health. Available online: https://gisresources.com/lidar-technology-monitoring-bridge-structure-defect-health/ (accessed on 5 February 2026).
38. Altabey WA. A Novel Framework to Identify Delamination Location/Size in BFRP Pipe Based on Convolutional Neural Network (CNN) Algorithm Hybrid with Capacitive Sensors. International Journal of Lightweight Materials and Manufacture. 2025; 8(3): 393–401. doi: 10.1016/j.ijlmm.2024.12.002
39. Cha YJ, Choi WO. Deep Learning-based Crack Damage Detection Using Convolutional Neural Networks. Computer-Aided Civil and Infrastructure Engineering. 2017; 32(5): 361–378.
40. Jang B, Kim M, Harerimana G, et al. Bi-LSTM model to increase accuracy in text classification: Combining word2vec CNN and attention mechanism. Applied Sciences. 2020; 10(17): 5841. doi: 10.3390/app10175841
41. Xu S, Zhang Q, Li W, et al. A novel method for circumferential joint localization and dislocation detection in subway shield tunnels based on point cloud intensity features and block strategy. Journal of Civil Structural Health Monitoring. 2026; 16(1): 4. doi: 10.1007/s13349-025-01045-2
42. Martinez-Cantin R. Bayesopt: A bayesian optimization library for nonlinear optimization, experimental design and bandits. Journal of Machine Learning Research. 2014; 15(1): 3735–3739.
43. Altabey WA. The fatigue damage monitoring of composite pipeline based on frequency domain analysis of electrical capacitance sensor system measurements. International Journal of Lightweight Materials and Manufacture. 2025; 8(6): 779–792. doi: 10.1016/j.ijlmm.2025.06.002
44. Hutter F, Hoos HH, Leyton-Brown K. Sequential model-based optimization for general algorithm configuration. In: Proceedings of the 5th international conference on Learning and Intelligent Optimization; 17–21 January 2011; Rome, Italy. pp. 507–523.
45. Bergstra J, Bardenet R, Bengio Y, et al. Algorithms for hyper-parameter optimization. In: Proceedings of the Advances in Neural Information Processing Systems; 12–14 December 2011; Granada, Spain. pp. 2546–2554.
46. Bergstra J, Yamins D, Cox D. Making a science of model search: Hyperparameter optimization in hundreds of dimensions for vision architectures. Proceedings of the 30th International Conference on Machine Learning. 2013; 28(1): 115–123.

47. Sun Z, Sun M, Siringoringo DM, et al. Predicting bridge longitudinal displacement from monitored operational loads with hierarchical CNN for condition assessment. Mechanical Systems and Signal Processing. 2023; 200: 110623. doi: 10.1016/j.ymssp.2023.110623
48. Ma Z, Choi J, Sohn H. Continuous bridge displacement estimation using millimeter-wave radar, strain gauge and accelerometer. Mechanical Systems and Signal Processing. 2023; 197: 110408. doi: 10.1016/j.ymssp.2023.110408